

# We are IntechOpen, the world's leading publisher of Open Access books Built by scientists, for scientists

4,800

Open access books available

122,000

International authors and editors

135M

Downloads

Our authors are among the

154

Countries delivered to

TOP 1%

most cited scientists

12.2%

Contributors from top 500 universities



WEB OF SCIENCE™

Selection of our books indexed in the Book Citation Index  
in Web of Science™ Core Collection (BKCI)

Interested in publishing with us?  
Contact [book.department@intechopen.com](mailto:book.department@intechopen.com)

Numbers displayed above are based on latest data collected.

For more information visit [www.intechopen.com](http://www.intechopen.com)



## Properties and Function of Pyomelanin

Charles E. Turick, Anna S. Knox, James M. Becnel,  
Amy A. Ekechukwu and Charles E. Milliken  
*Savannah River National Laboratory, Aiken, SC 29808*  
USA

### 1. Introduction

Melanin pigments are the most common pigments produced in nature and these complex biopolymers are found in species of all biological kingdoms. There are several categories of melanins which include eumelanins, pheomelanins and allomelanins. Eumelanins and pheomelanins are produced from oxidation of tyrosine or phenylalanine to *o*-dihydroxyphenylalanine (DOPA) and dopaquinone. Pheomelanin results from cysteinylolation of DOPA. Allomelanins include a heterogeneous group of polymers that include pyomelanin. Melanin biochemistry and synthesis has been reviewed previously (Plonka and Grabacka 2006). This chapter will focus on the properties and function of pyomelanin and their potential utility in biotechnology. Pyomelanin originates from the catabolism of tyrosine or phenylalanine (Lehninger, 1975) (Fig. 1). Complete breakdown of tyrosine to acetoacetate and fumarate requires the enzymes 4-hydroxyphenylpyruvic acid dioxygenase (4-HPPD) and homogentisic acid oxidase (HGA-oxidase). In the absence of HGA-oxidase, or if homogentisic acid (HGA) production exceeds that of HGA-oxidase activity, HGA is over-produced and excreted from the cell (Yabuuchi and Ohyama 1972; Ruzafa et al. 1994; Katob et al. 1995). Autooxidation and selfpolymerization of HGA then results in pyomelanin. In addition, deletion of the gene that encodes for HGA-oxidase results in hyper production of pyomelanin while deletion of the gene that encodes for 4-HPPD results in the inability to produce pyomelanin (Coon et al. 1994; Ruzafa et al. 1995). In humans with loss-of-function mutations in HGA-oxidase, pyomelanin (also known as alkapton or ochronotic pigment) forms in the urine due to the spontaneous auto oxidation of excess HGA (Beltrán-Valero de Bernabé, et al. 1999). This condition is known as alkaptonuria in humans and can result in arthritis in adults. Pyomelanin production in microorganisms often is associated with numerous survival advantages and was first characterized in bacteria among numerous species of the genus *Pseudomonas* (Yabuuchi & Ohyama 1972). Since then several fungi and a number of bacteria, especially in the  $\gamma$  Proteobacteria have been shown to produce pyomelanin.

### 2. Microbial exploitation of pyomelanin

Melanins are structurally similar to humic acids and thus have similar redox cycling properties (Menter & Willis, 1997; Stott & Martin, 1990). Although melanin pigments are thought to primarily function as a protection mechanism against ultraviolet (UV) radiation,

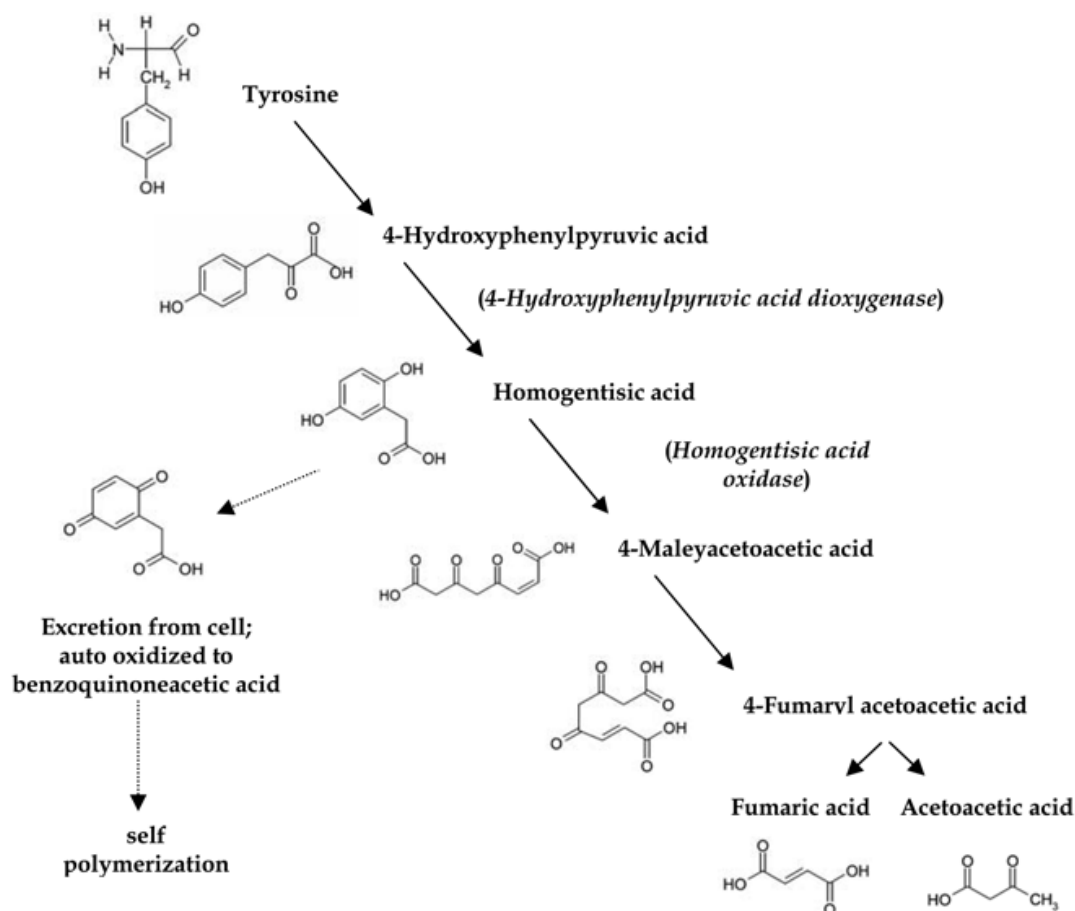


Fig. 1. Tyrosine degradation pathway showing tyrosine catabolism and pyomelanin production. Key enzymes in pyomelanin synthesis are in parentheses.

there is evidence that its useful properties to bacterial cells extend beyond this function. For instance, eumelanin has been reported to have cation exchange and metal sequestration properties (McLean et al., 1998; White, 1958). Cell cultures of the fungus *Aureobasidium pullulans* that produce eumelanin also show increased adsorption to numerous metals and tributyltin chloride relative to non-melanized cells (Gadd et al., 1990; Gadd and Mowll, 1985; Gadd et al., 1987). Uranium accumulation has also been reported in the eumelanin containing lichen *Trapelia involuta* when grown on uranium minerals (McLean et al., 1998). Hence, melanogenic organisms can be used in bioremediation and therefore have potential in biotechnology.

The properties of pyomelanin appear to be exploited by microorganisms for a survival advantage. Pyomelanin is formed abiotically outside the cell when excreted homogentisic acid autooxidizes to form benzoquinoneacetic acid. This is followed by self assembly into pyomelanin polymers. While pyomelanin at this point is a soluble exocellular pigment, it can also sorb to the cellular surface and thereby pigment the cell (Turick et al, 2003). The chemical structure of these polymers provides for a multifaceted biological utility such as; protection from light and oxidative stress, energy transduction and chemical reduction of soluble and solid phase metal oxides. For instance, pigmentation correlated with homogentisic acid production in *Legionella pneumophila* confers protection from light in the spectrum of 290-780 nm with a maximum at 635 nm (Steinert et al. 1995; Steinhert et al. 2001). Pyomelanin, like other melanin pigments is very reactive in the presence of reactive

oxygen species. Oxidative stress from peroxide is decreased in *Pseudomonas aeruginosa* as a result of pyomelanin production, a trait common in clinical isolates of *P. aeruginosa* from lungs of chronically infected patients (Rodríguez-Rojas et al. 2009). Similarly, pyomelanin produced by *Burkholderia cepacia* has been shown to scavenge superoxide radicals and may play a significant role in the survival during phagocytosis by pulmonary macrophages, an important pathogenic mechanism of persistent pulmonary infections (Zughaier et al. 1999). Iron chelation and reduction has been demonstrated with pyomelanin by *Shewanella algae* BrY (Turick et al. 2008 b) and has been linked to iron acquisition by *L. pneumophila* (Chatfield & Cianciotto, 2007). For iron assimilation to occur, Fe(III) must be reduced to Fe(II). The redox cycling properties of pyomelanin enable this process to occur.

When the redox cycling properties of pyomelanin are coupled to energy conservation by dissimilatory metal reducing bacteria, the rate of metal oxide reduction increases along with growth rates (Turick, et al. 2002; Turick, et al. 2003; Turick, et al. 2009). Similarly, dissimilatory metal reducing bacteria also are capable of using the pyomelanin they produce as a terminal electron acceptor (Turick, et al. 2002). This appears to only be the case of facultative anaerobes that experience daily fluctuations in oxygen levels. Pyomelanin production occurs during oxygen stress in the environment and may be a strategy to allow for increased electron transfer to inorganic terminal electron acceptors like Fe(III) oxides (Turick, et al. 2003; Turick, et al. 2009). Environmental concentrations of the precursors tyrosine or phenylalanine are likely sufficient in most locations to provide for enough pyomelanin production to significantly increase metal reduction rates (Turick, et al. 2009). However, pyomelanin production from cryptic growth also occurs in the absence of supplemental precursors in the laboratory (Turick, et al. 2009). Consequently, tyrosine or phenylalanine may not be required to be present in the environment for pyomelanin production to proceed, especially in biofilms where cell density is high.

The rate of exocellular electron transfer by dissimilatory metal reducing bacteria is enhanced by only small quantities of pyomelanin (femtograms per cell) due to the redox cycling nature of this polymer (Turick, et al. 2002; Turick, et al. 2009). Surface sorption of pyomelanin to the bacterial cell allows for its repeated use as an electron conduit (Turick, et al. 2003; Turick, et al. 2009). There is evidence of an optimum concentration on the cell surface whereupon; at higher concentrations electron transfer is slowed, possibly due to impedance from the polymeric structure (Turick, et al. 2009). Pyomelanin sorption onto bacterial surfaces may also have an indirect effect of increased electron transfer by trapping other soluble electron shuttles. The soluble electron shuttle riboflavin (Marsili et al. 2008) can be entrapped by pyomelanin polymers on the cell surface, which may result in the recycling of this electron shuttle (Turick, et al. 2009).

Given the nutrient and terminal electron acceptor limitations of biofilms, pyomelanin production would be considered a significant advantage for sustained metabolic activity in these environments. *B. cepacia* populations demonstrate an increase in the pyomelanin phenotype when grown in biofilms but not under pelagic growth. This biased generation of mutations is linked to mutagenic repair of double stranded DNA breaks caused by oxidative stress (Boles et al. 2004; Boles & Singh, 2008).

An understanding of the role of pyomelanin in microbial physiology and its genetic control will provide a better understanding of survival strategies utilized by specific pathogens linked to such diseases as cholera, cystic fibrosis and Legionnaires' disease. The multifaceted nature of pyomelanin provides opportunities for its exploitation for environmental and industrial

biotechnology. This chapter will address research into the possible structure and related properties of pyomelanin and its application in environmental and industrial biotechnology.

### **3. Material and methods**

#### **3.1 Pyomelanin production and isolation**

Bacterial pyomelanin was produced from reagent grade tyrosine (2g/l) in bacterial cultures of *Shewanella algae* BrY, concentrated through dialysis and stored as a dry (65°C) powder, as previously described (Turick, et al. 2002). HGA melanin (artificial pyomelanin) was produced by auto oxidation of reagent grade homogentisic acid in 1N NaOH, followed by concentration as above.

#### **3.2 In-situ production of pyomelanin**

Tyrosine (0.2 – 2 g) in 50 ml deionized water was sterilized and added to constructed soil columns in a uranium contaminated riparian zone and monitored over time for pore water metals at 10, 30, and 50 cm below surface using installed lysimeters (Turick, et al. 2008 a).

#### **3.3 Isolation of pyomelanin-producing bacteria**

Methods followed those reported previously (Turick, et al. 2008 a). In general most probable number assays incorporating lactate basal salts medium (Turick, et al. 2002) with and without 1g/l tyrosine were inoculated with fresh soil from the test plot (above) and incubated at 28°C for one month. Cultures from pigmented tubes were isolated on lactate basal salts agar with 2 g/l tyrosine for isolation of pigment producing bacteria. Pigments were characterized chemically, physically and through enzyme inhibition assays.

#### **3.4 Pyomelanin sorption studies**

Bacterial cultures grown in tryptic soy broth at 28°C were concentrated and washed through centrifugation 3 times and added as a cell suspension to test tubes with/without 2g/l sterile bacterial pyomelanin. Following incubation for 5 days at 28°C, cells were concentrated via centrifugation and washed 3 times as above, followed by analysis for pyomelanin as previously reported (Turick, et al. 2002).

#### **3.5 Electrochemistry**

Electrochemical measurements incorporating cyclic voltammetry were performed in the three-electrode geometry with a carbon paste working electrode, a Pt counter electrode (Bioanalytical Systems, BAS, West Lafayette, IN) and an Ag/AgCl, 3M NaCl reference (BAS), all immersed in the electrochemical cell. Potentials measured relative to Ag/AgCl, 3M NaCl. Potential sweeps originated in the positive direction for all cyclic voltammograms in this study, using a model 100B/A potentiostat (BAS) or a 2 channel Versastat potentiostat (Princeton Instruments, Trenton, NJ USA). Between each set of measurements using different cultures, the working electrodes were rinsed in sterile 50 mM phosphate buffered saline. For each culture analyzed, a CV of the washed bare electrode in PBS was recorded, which served as a no-cell control for the next series of voltammetry studies. Sweep rates from 100 to 1700mVs<sup>-1</sup> were conducted as above to determine surface or bulk phase electrochemical behavior of pyomelanin. These rates were analyzed and no significant peak distortions were detected at these rates. Studies incorporating dried (65°C) pore water from

in-situ pyomelanin production experiments involved analysis in nonaqueous liquid as previously described (Nurmi & Tratnyek, 2002) using a Pt working electrode (BAS). Between each set of measurements the working electrodes were rinsed in deionized water, followed by a methanol rinse, and sonication for 10 min in deionized water. Carbon paste electrode composites were constructed by mixing 10% (wt/wt) of pyomelanin, or anthraquinone disulfonate with carbon paste and inserting into electrode housings. Chronoamperometry of carbon paste and pyomelanin/carbon paste composite electrodes were conducted with a UV light source and poised potential of the electrodes at -700mV.

### 3.6 Fe(III) oxide reduction

Hydrous ferric oxide (50mM) was used to measure Fe(III) reduction kinetics in 1 g fresh soil in the presence of 10 ml carbonate buffer with H<sub>2</sub> as the electron donor, according to a previously described methodology (Turick, et al., 2002; 2003). Fe(II) was measured spectrophotometrically using the ferrozine assay as described elsewhere (Turick, et al., 2002). For analysis of bacterial cultures with/without sorbed pyomelanin, washed cells were added to anaerobic carbonate buffer containing hydrous ferric oxide, following the procedures above.

## 4. Structure and properties

In order for the properties of pyomelanin to be optimized for biotechnology, a better understanding of its structure is beneficial. Structural characterization of melanins has been elusive due to their size and complexity. Pyomelanin ranges from 10-14 kDa (Turick, et al. 2002) and is smaller than other melanin pigments. FTIR analyses of pyomelanin produced from the auto oxidation of HGA (HGA-melanin) (David, et al. 1996 and Turick, et al. 2003) reveal absorbance peaks consistent with the OH stretch of polymeric structures, aliphatic C-H bonds, aromatic C=C bonds conjugated with C=O and or COO<sup>-</sup> groups as well as phenolic OH groups. HGA-melanin provides a good starting point in beginning to determine the structure and function of microbial pyomelanin. The relative purity of HGA melanin provides for a consistent structure because microbial pigments often contain metabolic residues such as proteins, amino acids and carbohydrates (David, et al. 1996).

Based on FTIR data and other previous results, (David et al) there are several possible polymeric structures resulting from HGA auto oxidation and polymerization (Fig.2). Combining FTIR data and computational chemistry analysis allows us to predict some functional aspects of HGA-melanin and then correlate the predictions to experimental results.

The electron transfer properties of L-DOPA melanin pigments have been demonstrated through the coupling of hydroxybenzene depigmenting-compound oxidation to ferric cyanide reduction (Menter & Willis, 1997). The electron transfer properties of melanin polymers, including pyomelanin, also constitute a mechanism of electron transfer to solid electron acceptors like metal oxides (Ellis & Griffiths, 1974, Turick et al. 2002; 2003; 2009) and electrodes (Turick, et al. 2009). Based on this information, the structure that most likely will provide for optimum electron transfer capacity is structure B in Figure 2. This quality is due largely to the presence of quinones. Figure 3 illustrates the HGA melanin electron density iso-surface (at 0.2 e/<sup>Å</sup><sup>3</sup>) colored by susceptibility to radical attack (red = high, blue = low).

Going by these, the CH<sub>2</sub>COOH group is probably not attacked, and that still leaves the ring and the OH groups. An expected increase in electron transfer potential exists in structure B in Figure 2, compared to the other structures in Figures 2&3. Based on the computational analyses, an alternating structure would possess minimal electron transfer properties due to

the absence of quinones and hence is not a likely structure of HGA melanin or microbial pyomelanin.

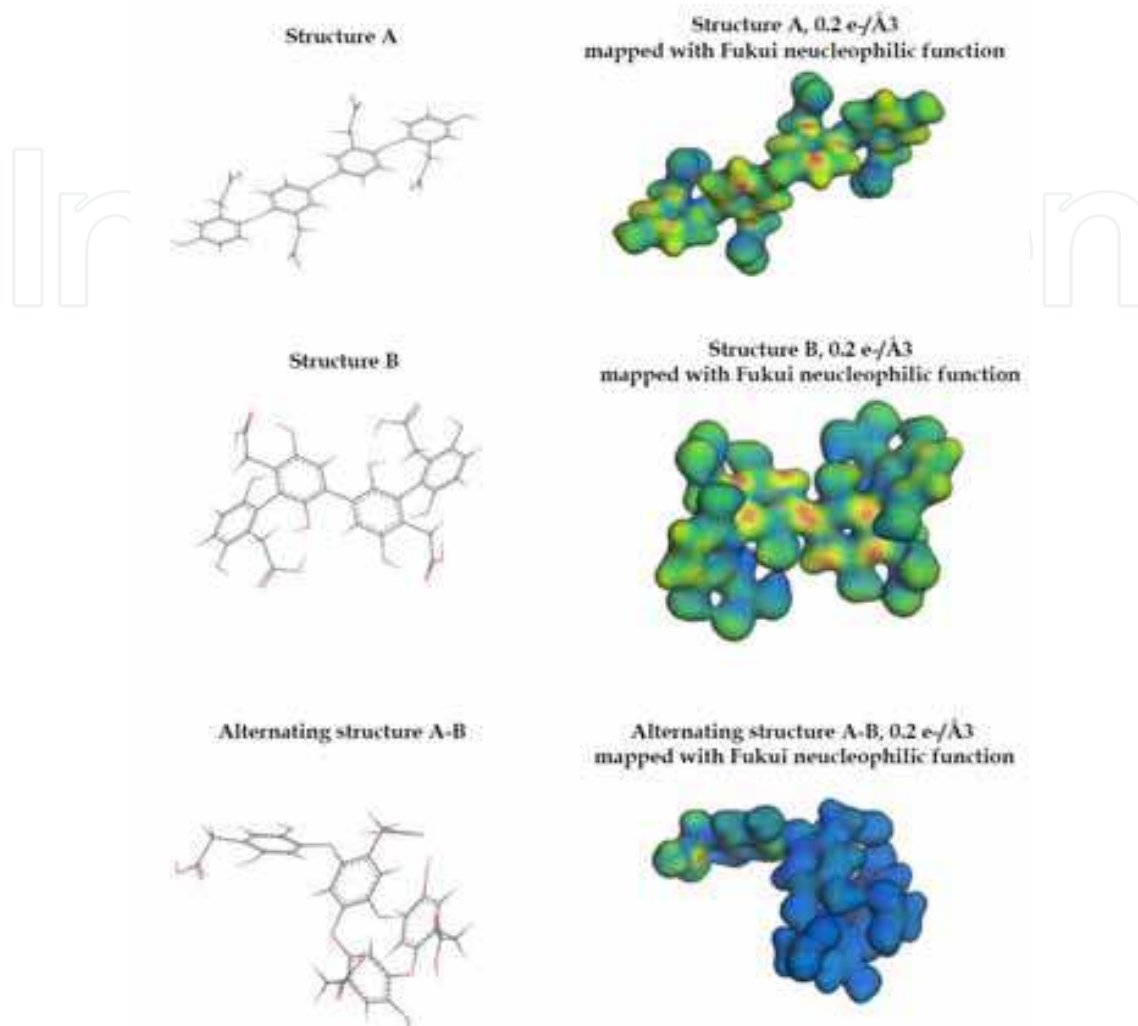


Fig. 2. Possible linear polymer structure of HGA-melanin. Line structures (left) are derived from David et al. (1996) and their corresponding simulated 3D structure mapped with Fukui nucleophilic function (right). The colorations are electrophilic Fukui Function values, for radical attack describes the relative ease of transferring a small amount of charge from the highest occupied molecular orbital to the lowest unoccupied molecular orbital.

Computations for HGA-melanin have shown the increased availability of conducting electrons in the quinone forms of the pyomelanin. Two possible structures presented in David, *et. al.* (1996) and Figure 2 are analyzed along with a quinone-analog structure. In order to confirm our computational analyses of the electrochemical properties of pyomelanin in response to radical attack we monitored the current response of a pyomelanin/carbon paste electrode compared to carbon paste alone in the presence of UV light. L-DOPA melanin interacts with UV light by offering protection from harmful radical formation. Microbial pyomelanin also displayed an electrochemical response to UV light when combined with a carbon paste electrode at a 1:10 wt/wt ratio of carbon paste (Fig. 4). These results demonstrate that pyomelanin reacts with UV light in a similar fashion as L-DOPA melanin. These data also offer further evidence that pyomelanin is composed of multiple quinone moieties.

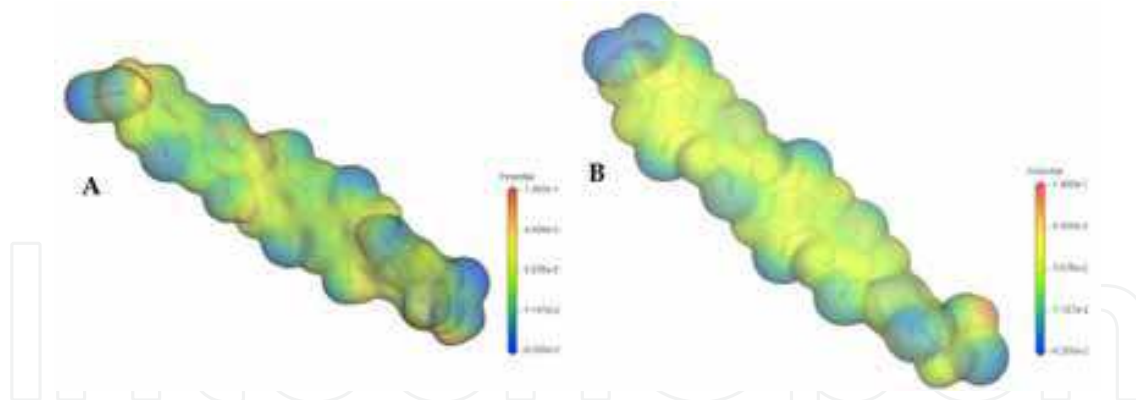


Fig. 3. HGA melanin electron density iso-surface (at  $0.2 \text{ e}/\text{\AA}^3$ ) colored by susceptibility to radical attack (red = high, blue = low). Structures are partially oxidized (semiquinone) (A) and fully oxidized (quinone) (B). The colorations are electrophilic Fukui Function values, for radical attack describes the relative ease of transferring a small amount of charge from the highest occupied molecular orbital to the lowest unoccupied molecular orbital.

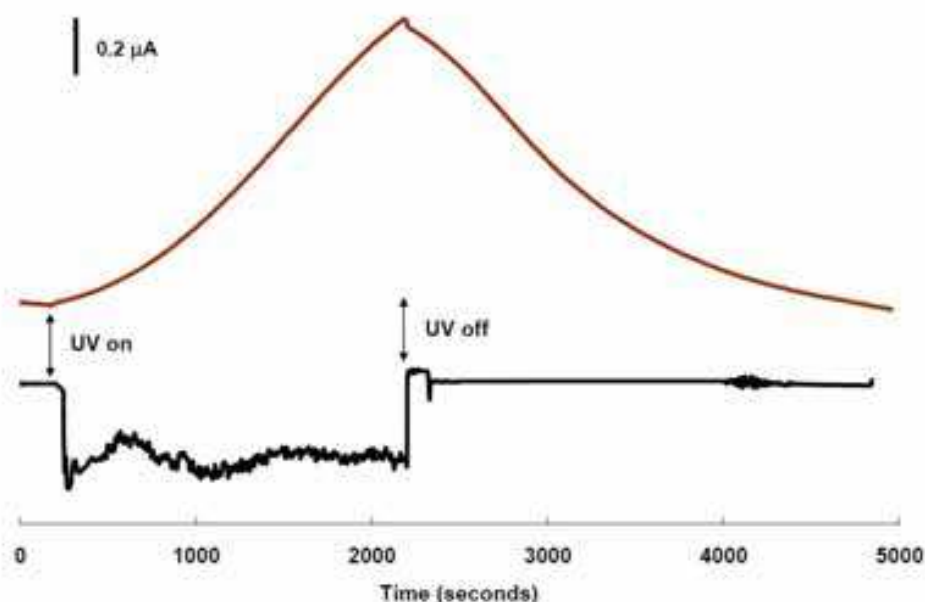


Fig. 4. Pyomelanin Response to UV Light ( $365 \text{ nm}$ ,  $9100 \text{ mW}/\text{cm}^2$ ). Pyomelanin also displayed an increased current in response to UV light when combined with a carbon paste electrode at a 1:10 wt/wt ratio of carbon paste. Electrodes were poised at  $-700 \text{ mV}$  (vs  $\text{Ag}/\text{AgCl}$ ) throughout the study.

By examining a short, five-ringed segment of the proposed structure, QM calculations show that as the structure becomes more quinone-like, there is a higher density of electrons near the Fermi level, indicating more electrons are available for conduction. In Figure 5, Structure A has no quinone-like character, Structure B hydro-quinone groups that could become oxidized to quinones, and Structure C is Structure B oxidized to a full quinone state; all three structures have a net charge of 0. The figure shows the increase in the density of conducting electrons as we move to the quinone-like structure.

Figure 6 shows a structure of a small, 5kDa pyomelanin segment (of the quinone structure depicted in Figure 5C. after simulated annealing with the COMPASS force field. This simple



simulation illustrates that the quinone-analog of the pyomelanin structure has a tendency to form a spiraled structure. To verify the presence of quinones, studies incorporating cyclic voltammetry were conducted to determine if the electrochemical behavior of pyomelanin was similar to a 2-step oxidation followed by a 2 step reduction of the model quinone anthraquinone-2,6-disulfonate (AQDS). A 2-step oxidation followed by a 2 step reduction was determined for AQDS as well as pyomelanin (Fig. 7) and thus providing strong evidence of the presence of quinones in the pyomelanin structure, as well as corroborating previous findings employing wet chemistry techniques (Turick, et al. 2003).

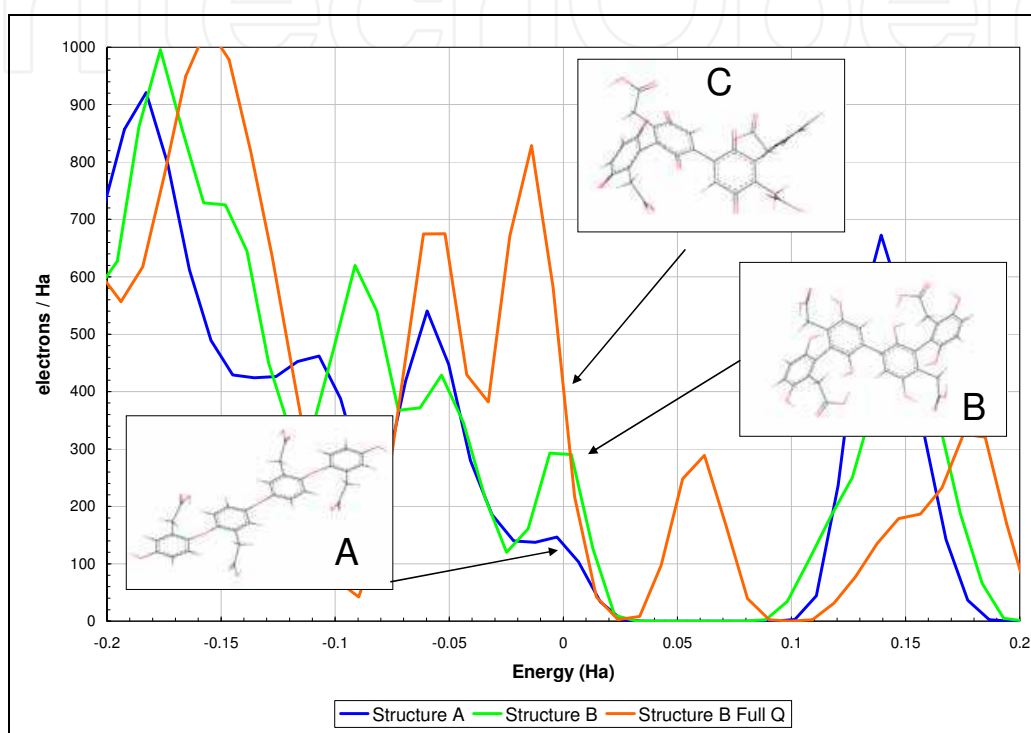


Fig. 5. Superimposed density of states for three postulated structures of HGA-melanin from Figure A. A significant difference is demonstrated here between the quinone state (C) and the hydro-quinone state (B).

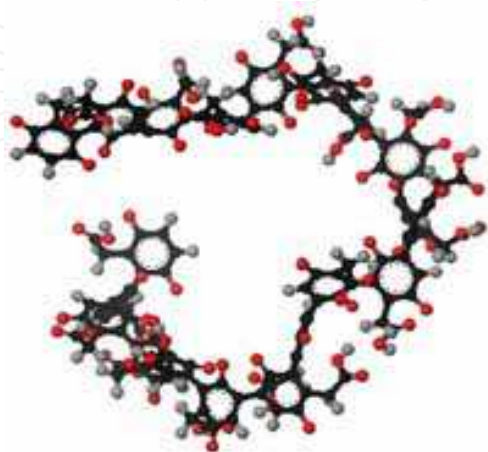


Fig. 6. Structure of a small, 5kDa pyomelanin segment of the quinone structure depicted in Fig.5-C after simulated annealing with the COMPASS force field.

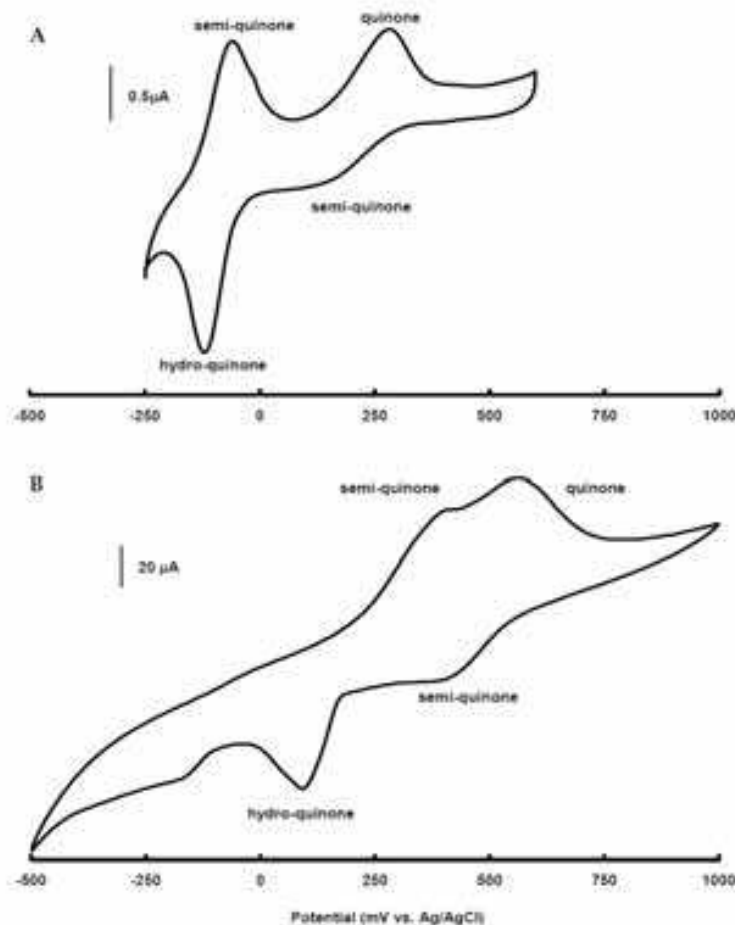


Fig. 7. Cyclic voltammetry of AQDS and pyomelanin. AQDS (A) and pyomelanin (B) were mixed individually in a 1:10 ratio (wt/wt) with carbon paste and analyzed in 50 mM phosphate buffered saline at pH 2. Scans began at  $-500$  mV and moved in the positive direction at  $25$  mV/s. A 2-step oxidation (upper peaks) and 2-step reduction (downward peaks) are indicative of quinones.

## 5. Biotechnological applications

### 5.1 Biogeochemistry: metal transformation and redox manipulation

The metal binding and electron shuttling properties of pyomelanin offer a means of altering the biogeochemistry of specific environmental sites provided the conditions are appropriate for pyomelanin production as well as conducive to electron transfer and metal retention in the soil. Supplementation of soil with the chemical precursors tyrosine and/or phenylalanine was successful in resulting in pyomelanin production (Turick, et al. 2008 b). Due to the long-term affects of pyomelanin on the environment, a one-time application of these carbon sources may prove cost effective in many cases. Environmental conditions that may limit the production of pyomelanin include Fe(II) availability. The presence of Fe(II) in laboratory studies demonstrated decreased rates and degrees of pyomelanin production as a function of Fe(II) present (Turick, et al. 2008 b). While 4-HPPD is required for pyomelanin production and Fe(II) is required for this enzyme, increased Fe(II) concentrations decrease 4-HPPD activity (Lindstedt, et al. 1977). Similarly, we have found the rate of pyomelanin production to also follow a similar trend relative to Fe(II) in laboratory studies (Fig. 8)

These results suggest that pyomelanin production will be low in soils with higher concentrations of bioavailable iron. It is interesting to note that along with evidence that pyomelanin is used in Fe(II) acquisition, Fe(II) concentrations in the environment may limit the activity of 4-HPPD and as a result minimize pyomelanin production when Fe(II) is in abundance.

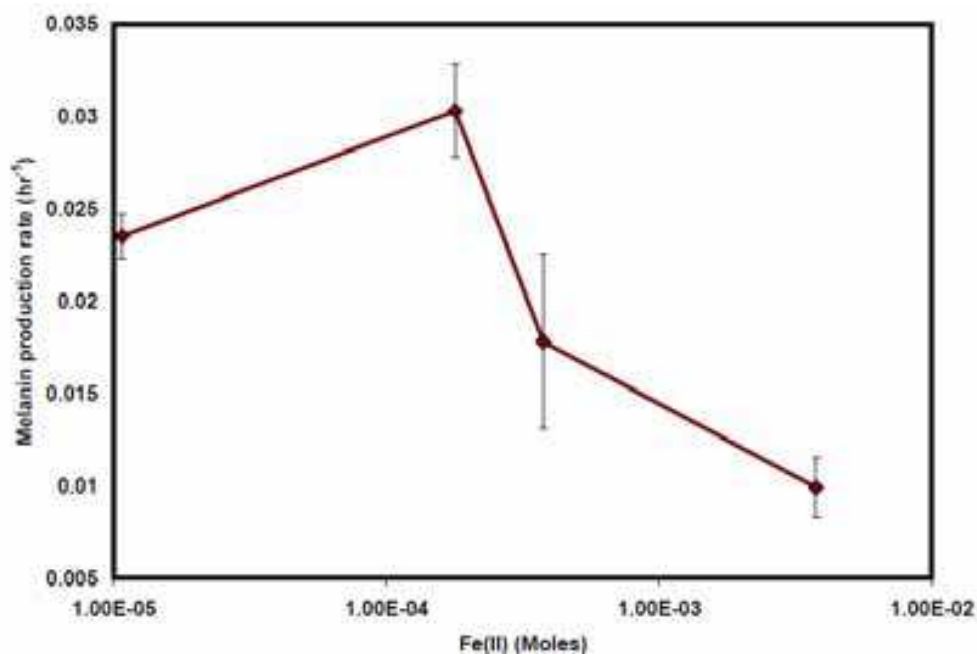


Fig. 8. Pyomelanin production rates by *S. algae* BrY in relation to Fe(II) concentrations. Fe(II) concentrations drastically inhibit the rate of pyomelanin production above 0.5 mM Fe(II).

The presence of naturally occurring bacteria capable of pyomelanin production eliminated the need to augment the soil with pure cultures of allochthonous pyomelanin producers (Turick, et al. 2008 b). A pyomelanin producing strain (Fig. 9) previously isolated from uranium contaminated soil (Turick, et al. 2008 b) has since been tentatively identified as *Bacillus mycoides* through fatty acid methyl ester analysis. Little is known however about the abundance of pyomelanin production in the environment. Since bacteria need only small quantities of this polymer to enhance their electron shuttling capacity, the low detection limit required to identify environmentally relevant quantities marginalizes a direct analytical chemical approach. However, given that numerous strains of soil bacteria are known to produce pyomelanin and if the rate of mutation of the HGA-oxidase gene is similar in bacteria to that in humans (1:100,000 - 250,000) (Zatkova, et al. 2000), pyomelanin-producing bacteria may be ubiquitous in the environment.

If present in a particular environment, pyomelanin producers may be too low in number to contribute to significant electron transfer and hence metal transformation. However, sufficient supplementation of tyrosine (1-10 mM) to the soil resulted in significant production of pyomelanin production. The result was a dramatic increase of the redox properties of the soil as determined through Fe(III) oxide reduction assays and electrochemistry (Fig. 10). With H<sub>2</sub> as the electron donor, Fe(III) reduction, as measured as Fe(II) evolution was greater in soils with pyomelanin compared to equal molar concentrations of the carbon and energy source lactate. Similarly, the redox activity as measured by cyclic voltammetry was greater in pyomelanin containing soils. Cyclic

voltammograms revealed two distinct oxidation (upward) peaks and reduction (downward) peaks with pyomelanin-containing soils whereas only one smaller redox couple was detected in controls. Peaks less than  $-750$  mV were likely due to solvent breakdown.

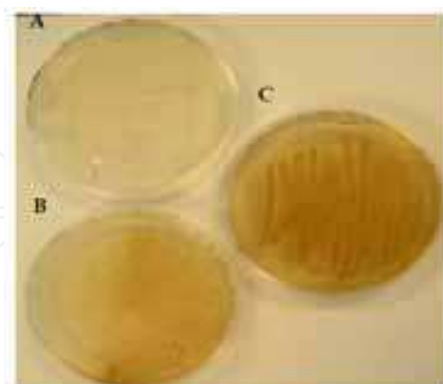


Fig. 9. Growth of melanin producing isolate from uranium contaminated soils. Results after 1 week growth on lactate basal salts medium. without tyrosine (A) and with tyrosine (B). Redish-brown coloration is a result of partial catabolism of tyrosine. More intense pigmentation was evident after 2 weeks growth on the same medium (C). Redish brown pigment was identified as pyomelanin.

Laboratory studies suggest that pyomelanin reduction may occur by other soil bacteria that are not pyomelanin producers. The sorptive capacity of pyomelanin to bacterial cells was not limited to pyomelanin producers (Table 1) and all bacterial strains tested under anaerobic conditions ( $50\%H_2/50\%N_2$ ), in the presence of pyomelanin, demonstrated increased Fe(III) oxide reduction with  $H_2$  as electron donor.

#### Fe(III) oxide (mM) reduced in 72h

<i>Species</i>	Control	With pyomelanin	Pyomelanin sorbed ( $\mu\text{g/l}$ )/ $10^8$ cells/ml
<i>B. cereus</i>	0.02 (0.005)#	0.25 (0.02)	1.8 (0.7)
<i>V. angullarium</i>	0.02 (0.004)	0.12 (0.02)	ND*
<i>P. putida</i>	0.02 (0.001)	0.30 (0.03)	0.7 (0.4)
<i>M. luteus</i>	0.01 (0.005)	0.09 (0.01)	0.4 (0.2)
<i>E. coli</i> K-12	0.02 (0.009)	0.09 (0.01)	1.8 (0.2)
<i>P. aeruginosa</i>	0.01 (0.011)	0.04 (0.02)	0.2 (0.05)

# standard deviation in parenthesis; \* ND= not determined.

Table 1. Pyomelanin sorption to bacteria and resultant increased metal reduction capacity

The bacteria evaluated in Table 1 do not couple energy conservation and growth to metal reduction and hence do not typically play a significant role in metal transformation in the environment. However a small degree of metal reduction does occur by these bacteria. Metal reduction in this case is often viewed as a sink for excess reducing power of microorganisms or part of assimilatory Fe(III) reduction (Ehrlich 2002, & Schröder et al, 2003). However the proportion of bacteria capable of metal reduction, but not coupled to growth, would be expected to be far greater than dissimilatory metal reducers in

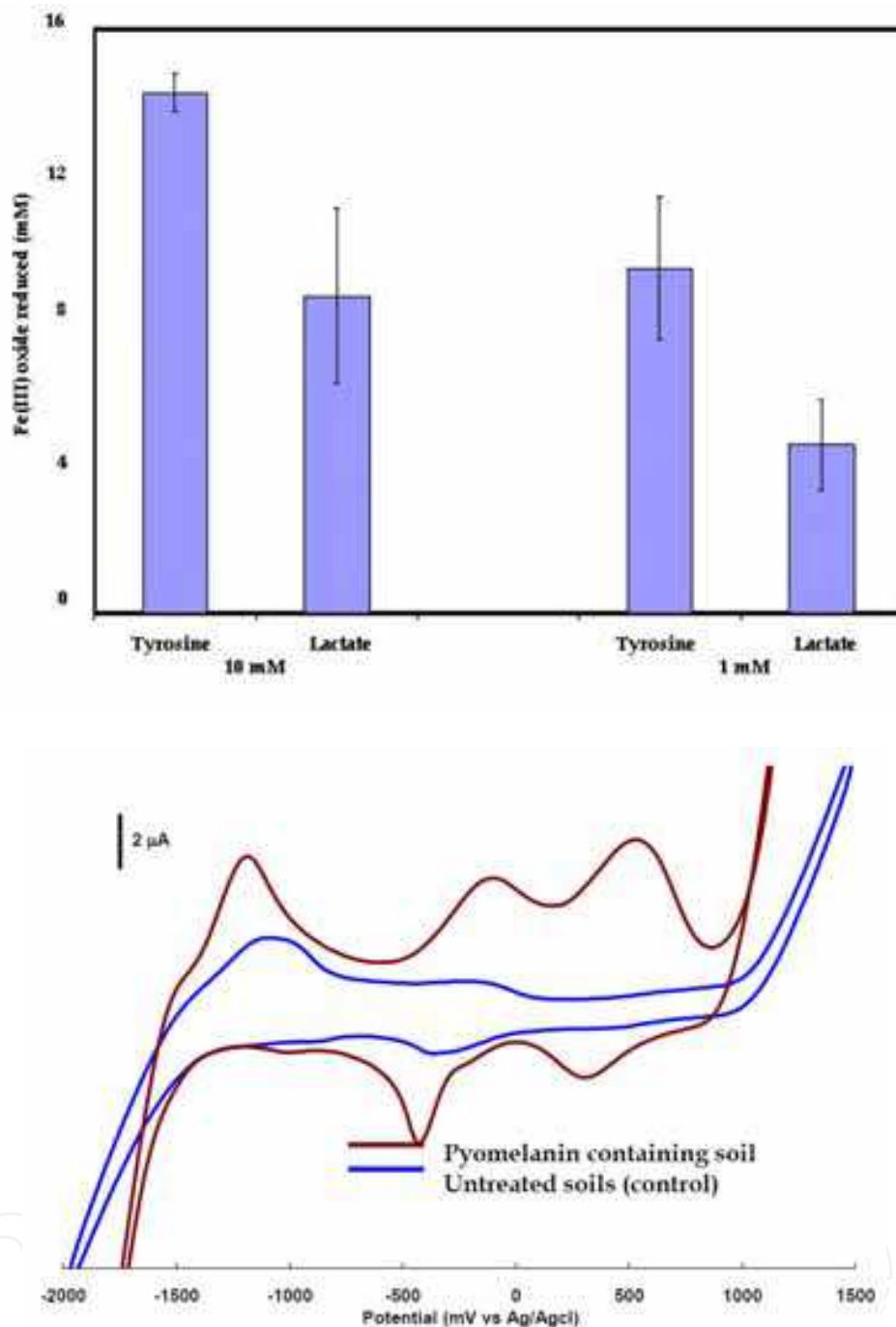


Fig. 10. Increased electron transfer capacity of soil with pyromelanin produced in-situ. Soils treated with tyrosine which resulted in pyromelanin production had an increased capacity for reduction of supplemental Fe(III) oxide under anaerobic conditions compared to equal molar concentrations of lactate after exposure to hydrogen (electron donor) for one week (top). Cyclic voltammograms (bottom) of dried (65°C) soils in DMSO also demonstrated increased redox activity of pyromelanin containing soils (brown) compared to controls (blue). Voltammograms were obtained with a Pt working electrode and Pt wire as counter electrode and the reference electrode was Ag/AgCl. Scan rate was 100 mV/s beginning at -2V and proceeding in the positive direction.

many subsurface environments. Indeed, dissimilatory metal reducing bacteria may be in very low numbers or even absent in some environments (Lehman, et al. 2001). Fe(III) reduction was also reported by the yeast *Cryptococcus neoformans* (Nyhus, et al., 1997) and is facilitated by extracellular melanin for Fe(III) reduction but does not appear to be coupled to energy conservation or growth, instead the resultant Fe(II) is assimilated. A similar mechanism was reported for *L. pneumophilla* where pyomelanin produced by this organism associates with the cell surface and reduces Fe(III), resulting in Fe(II) assimilation (Cianciotto, et al 2002). The action of various complexing agents, including quinones, to facilitate Fe(III) reduction for assimilation by bacteria are linked to dehydrogenase activity (Schröder et al, 2003).

Previous work has also demonstrated the ability of bacteria to reduce a variety of quinone-containing compounds, ultimately increasing the rates of azo dye reduction (Rau, et al. 2002). The quinone-reducing bacteria in the study of Rau et al. represented considerable diversity and included lactic acid bacteria, high and low GC Gram positive bacteria, as well as bacteria from the  $\alpha$ ,  $\beta$ , and  $\gamma$ -Proteobacteria, including *Escherichia.coli* K12. Therefore one should expect quinone reduction by soil bacteria to be common. Hence, the role of quinone-containing compounds as electron shuttles for non-dissimilatory metal reducing bacteria offers another possibility to control redox conditions and metal transformations in the environment. Based on these studies, pyomelanin production in-situ has the potential to accelerate metal reduction by a broad range of soil bacteria even though this process is not linked to energy conservation and growth.

## 5.2 Biogeochemistry: metal immobilization

The biotechnological use of pyomelanin is being explored for accelerated in-situ metal contaminant immobilization. The stimulation of pyomelanin production in-situ allows for inorganic contaminant immobilization due to metal binding and mineral sorption properties of pyomelanin. The properties of metal binding and surface sorption of pyomelanin were applied to field studies for uranium immobilization through the formation of a ternary structure with soil components (Turick, et al. 2008 b). Our previous work focused on the mechanisms of uranium complexation with pyomelanin and subsequent pyomelanin sorption to clay and mineral particles. This approach, which includes the addition of tyrosine to surface soils, results in production of pyomelanin pigments followed by a decrease in pore-water uranium concentrations. Through a one-time supplementation of tyrosine, uranium is immobilized for at least 13 months relative to controls. Follow-on studies were conducted to determine how in-situ pyomelanin production affected sorption phenomena in the soil.

Uranium immobilization was quantified by determining the partition coefficient of various treatments at different depths. The metal partition coefficient ( $K_d$ ; also known as the sorption distribution coefficient) is the ratio of sorbed metal concentration to the dissolved metal concentration. Uranium  $K_d$  values were highest with the tyrosine treated soils (Table 2). The resulting conversion of tyrosine to pyomelanin played a significant role in retarding uranium transport from the soil. While lactate addition also increased  $K_d$  values, they were not as high as the tyrosine treatments. Lactate is a carbon and energy source for bacteria and hence likely contributed to microbial activities that influenced, to some degree, the biogeochemical behavior of uranium. This effect was not as long lasting as that of the tyrosine amended soils.

Depth (cm)	Control	10 mM Lactate	10 mM Tyrosine
After 1 month			
10	9,954	28,198	47,569
30	6,359	17,154	36,744
50	4,394	15,133	26,592
After 13 months			
10	4,151	15,789	16,503
30	8,592	5,022	13,187
50	3,514	3,629	8,810

\*= ml/g

Table 2.  $K_d^*$  values for uranium resulting from various soil treatments

The one-time, in-situ stimulation of pyomelanin production resulted in a considerable impact on uranium mobility over one year, down to at least 50 cm. We also examined other metals to get a better idea of the effect of this metal immobilization approach. Figure 11 illustrates the affect of pyomelanin production on molybdenum, lead, bismuth and arsenic one month and 13 months after treatment ensued. Pore-water metal concentrations in general were higher for the controls compared to the pyomelanin containing soil.

The mechanism of pyomelanin sorption to soil and its related effects on the sorptive capacity of metal ions was also examined one month after pyomelanin stimulation began. XRF data of control soils demonstrated that uranium, calcium, nickel and zinc displayed a strong correlation to iron and manganese oxides. This correlation did not exist to the same degree in the presence of pyomelanin (Fig. 12). A possible explanation for this phenomenon is that pyomelanin sorbed easily to clays at the subsurface pH of 3.9 – 5.2. Previously we demonstrated that pyomelanin sorbes readily to illite and goethite at pH 4. The greater abundance of clay than iron or manganese minerals in this soil likely contributed to the difference in metal sorption indicated in our XRF data. Interestingly, changes in metal sorption did not necessarily increase metal immobilization in all cases. Nickel and zinc in particular did not demonstrate any changes in metal concentration in the pore water.

This work demonstrated the biotechnological use of bacterial biopolymers in accelerated in-situ metal contaminant immobilization. The stimulation of pyomelanin production in-situ allowed for inorganic contaminant immobilization due to metal binding and mineral sorption properties of pyomelanin. Similarly, the electron transfer capacity of pyomelanin accelerates soluble and solid phase metal reduction. The ability for pyomelanin to be sorbed onto bacterial surfaces may also accelerate electron transfer between a significant portion of the soil microbial population to contaminating metal oxides.

### 5.3 Microbial production of electric current

The ability of some bacteria to access solid mineral oxides as terminal electron acceptors has elicited interest in understanding mechanisms of bacterial electron transfer to solid terminal electron acceptors, including electrodes. Bacterial production of electric current results when an anode is used as a sink for electrons produced through microbial physiological activities. This phenomenon is being exploited for electricity production through microbial fuel cells (Drapcho, et al. 2008) sensors, and new methods for studying microbial physiology. Because pyomelanin increases the rate of electron transfer by bacteria that transfer

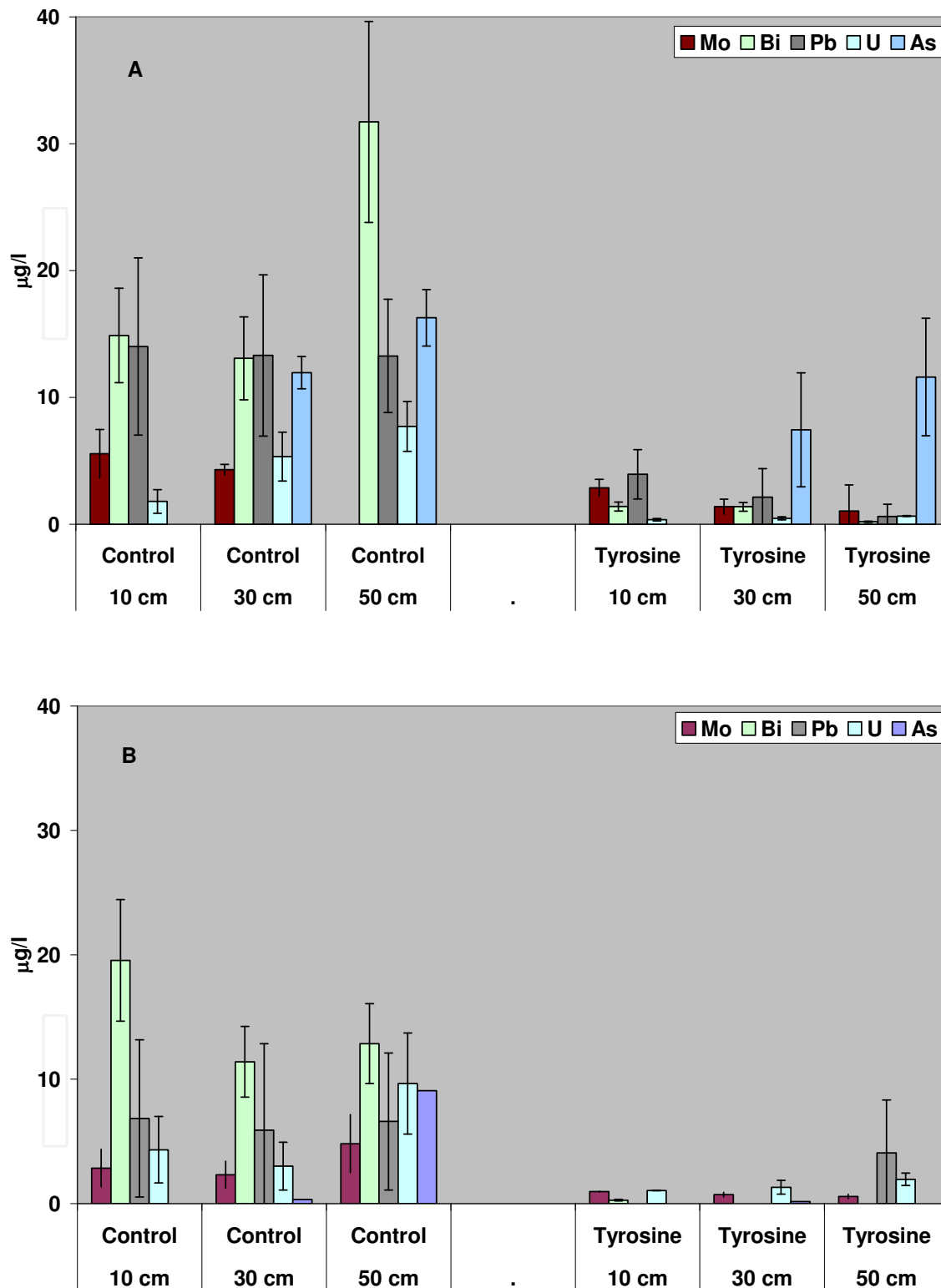


Fig. 11. Affect of pyomelanin production on molybdenum, gold, lead, bismuth and arsenic one month (A) and 13 months (B) after treatment ensued. Pore-water metal concentrations in general were higher for the untreated controls compared to the tyrosine treatments that resulted in pyomelanin production in soil.



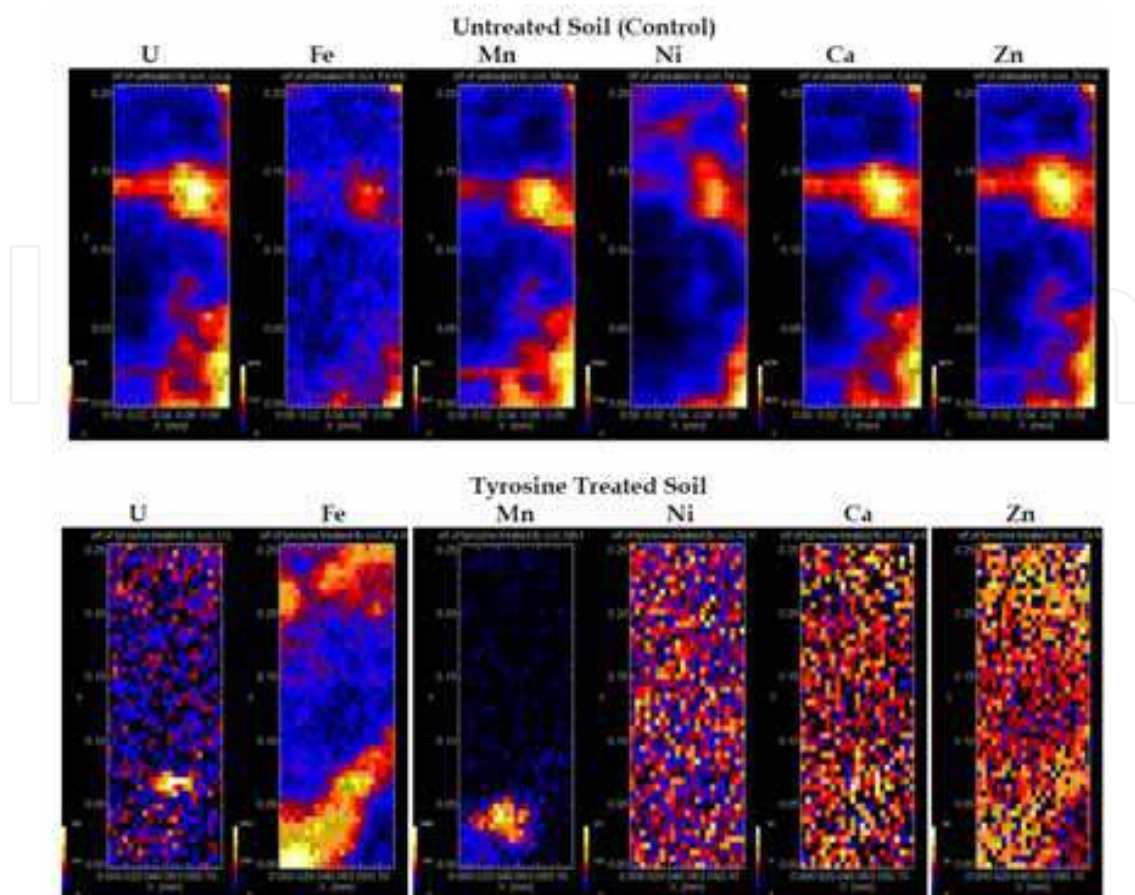


Fig. 12. XRF data of control soils demonstrate that uranium, calcium, nickel and zinc displayed a strong correlation to iron and manganese oxides. This correlation did not exist to the same degree in the presence of pyomelanin in tyrosine treated soils.

electrons to insoluble Fe(III) minerals, these microorganisms also demonstrate increased rates of electron transfer to electrodes in microbial fuel cells, resulting in increased current for electricity production. The dynamics of electron transfer from bacterial cells as examined through electrochemistry demonstrates the utility of pyomelanin as an electron conduit from the cell to the anode.

The bacteria *S. oneidensis* MR-1 is a model dissimilatory metal reducer that also produces pyomelanin. Through directed mutagenesis the gene that encodes for HGA oxidase (*hmgA*) was deleted resulting in a pyomelanin hyperproducer ( $\Delta hmgA$ ) and in another strain, the gene encoding for 4-HPPD (*melA*) was deleted resulting in a pyomelanin deficient strain ( $\Delta melA$ ) (Turick, et al. 2009) (Fig. 13). These strains were employed in the following studies to understand the roles of pyomelanin in electron transfer to anodes. The sorptive nature of pyomelanin offers an advantage as a potential electron shuttle that is associated to the bacteria surface and the anode. To confirm this, electrochemistry studies employing cyclic voltammetry were conducted at various sweep rates (Fig. 14) with a pyomelanin hyperproducing strain *S. oneidensis*  $\Delta hmgA$ . When the peak current is plotted against the scan rates, if the data demonstrate a high linear correlation, this indicates surface associated electron transfer, while a high correlation to the log of the scan rates indicates electron transfer in the bulk phase or a soluble electron shuttle. The data from Fig. 14 are indicative of surface associated electron transfer. The redox couple labeled as Peak 2 (ox. and red.) in

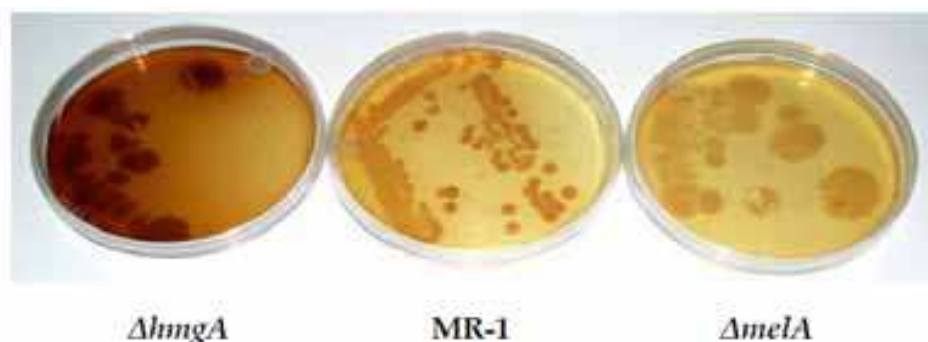


Fig. 13. Strains of the model dissimilatory metal reducing bacteria *S. oneidensis* used in these studies. Through directed mutagenesis, a pyomelanin hyper producing mutant ( $\Delta hmgA$ ) and a pyomelanin deficient mutant ( $\Delta melA$ ) were generated and used in this study to determine the role of pyomelanin on electrogenic biofilms of the wild type strain *Shewanella oneidensis* MR-1.

Fig. 14 were defined previously as pyomelanin.(Turick et al 2009,). These data coincide with previous work (Turick, et al. 2003) demonstrating that pyomelanin is associated with the bacterial surface. Riboflavin is a soluble electron shuttle produced by *S. oneidensis* (Marsilli, et al. 2009) and is also associated with and entrapped by pyomelanin (Turick, et al. 2009). Its electrochemical signature is described in Figure 4 as Peak 1.

The three strains of *S. oneidensis* (above) were grown in TSB in the presence of sterile patterned electrodes poised at 400 mV (vs Ag/AgCl) to determine the affect of pyomelanin production on electron transfer to an anode. The patterned electrodes used had a very hydrophobic working electrode (diameter, 2mm). Cells were grown at 28°C with enough stirring to keep the cells in suspension but to also maintain microaerobic conditions. Cell densities were similar in all cultures analyzed throughout the study. Current was monitored over time and stabilized after 72 hrs. Electrodes were examined microscopically at the termination of the experiment and no biofilms were detected on the hydrophobic working electrode. This indicated that electrons were passed to the electrodes by the suspension culture and not by biofilms growing on the electrodes. Current production was relative to pyomelanin produced by these cultures (Turick, et al. 2009) (Fig. 15), demonstrating the utility of pyomelanin as an electron conduit.

In order to study current production from biofilms, cultures were grown as above but on identical graphite rods as working electrodes to provide a suitable surface for biofilm development. The working electrodes were immersed 5 cm into the medium to provide sufficient surface area to the culture. These studies demonstrated similar results with respect to increased current production by the pyomelanin hyper producer when compared to the pyomelanin deficient strain. During establishment of biofilms,  $\Delta hmgA$  demonstrated increased current production at the termination of aeration (Fig. 16-A). Pyomelanin production occurs during oxygen stress and during this time the  $\Delta hmgA$  culture broth began to turn redish brown (indicative of pyomelanin) compared to the  $\Delta melA$  culture. TSB has sufficient tyrosine and phenylalanine to support pyomelanin production (McCuen, 1988). Following establishment of a biofilm on the electrode and current production the electrodes were rinsed gently in sterile phosphate buffered saline (pH 7) and then placed in clean phosphate buffered saline for cyclic voltammetry analysis. These analyses demonstrated enhanced current production by the pyomelanin hyper producer with a current response similar to that of pyomelanin (Figure 16-B).

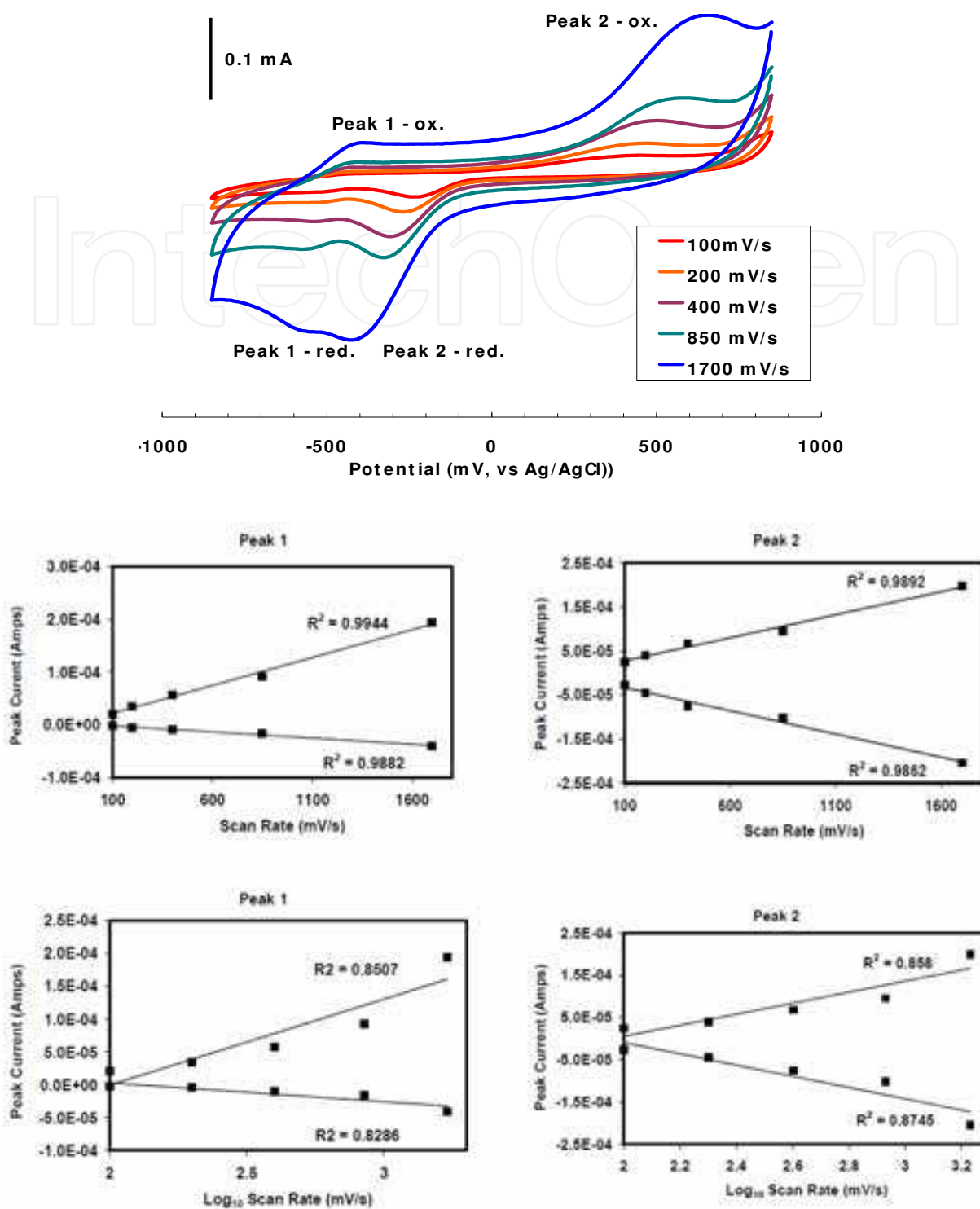


Fig. 14. Determination of surface associated, bacterial electron transfer by pyomelanin. Cyclic voltammetry conducted at various scan rates (top graph) was used to determine if electron transfer to the electrode by the pyomelanin over producer occurred at the cell surface or in the bulk phase. In these scans, oxidation peaks are upward and reduction peaks are downward. Peak currents plotted against scan rates demonstrated a higher linear correlation as compared to a logarithmic correlation, which would demonstrate surface associated electron transfer.

Directly following the previous study, the graphite rod working electrodes with biofilms were transferred to TSB (as above) and incubated for 4 days to allow further biofilm growth followed by a change to fresh TSB. The fresh static, microaerobic medium [dissolved oxygen =  $1.7(\pm 0.09)$  nMmL<sup>-1</sup>] demonstrated increasing current production from the  $\Delta hmgA$  culture relative to the pyomelanin deficient strain  $\Delta melA$  (Fig. 16C). Cyclic voltammetry performed on the rinsed working electrodes demonstrated significant differences between the two strains where  $\Delta hmgA$  revealed a greater current density and charge capacity as well as several redox couples, indicative of pyomelanin.

Upon termination of this study, biofilm thickness on the electrodes (determined with confocal microscopy) was similar for both cultures at the bottom of the 5 cm electrode but thicker at the top (air/medium interface) (Fig. 17). Current production in microaerobic environments exceeds that of strict anaerobic conditions and could be a result of production of electron shuttles under microaerobic conditions (Mohan, et al. 2008). This could explain why the biofilm of the pyomelanin hyper producer was thicker at the medium surface but the pyomelanin deficient strain had consistent biofilm thickness along the working electrode.

The only difference between these two strains was the ability to make pyomelanin and these results demonstrate the contribution of pyomelanin to electron transfer to solid terminal electron acceptors. *S. oneidensis* has numerous mechanisms for electron transfer to solid terminal electron acceptors and is evident with current production from  $\Delta melA$ . While it is conceivable that  $\Delta melA$  utilized other electron shuttle mechanisms to a greater extent in the absence of pyomelanin production, the overall differences in current production between these two strains demonstrated the utility of pyomelanin as an electron conduit for bacterial growth.

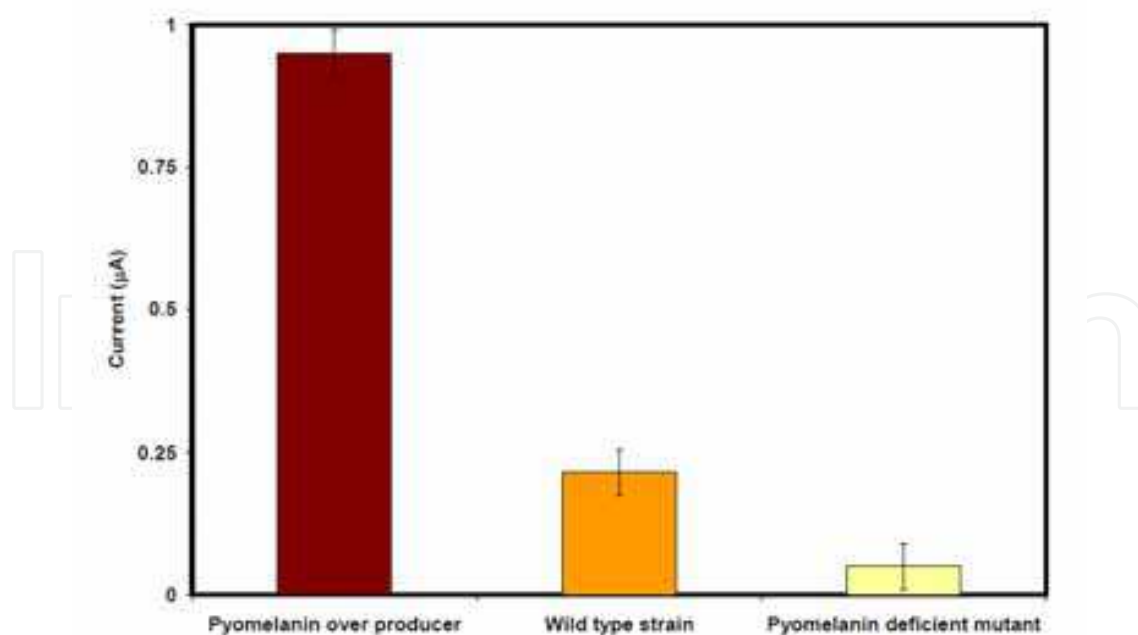


Fig. 15. Role of pyomelanin production on electric current production. Using a patterned composite electrode with hydrophobic graphite as working electrode stirred pelagic bacterial cultures demonstrated increased electron transfer, measured as electric current production as a function of pyomelanin production.

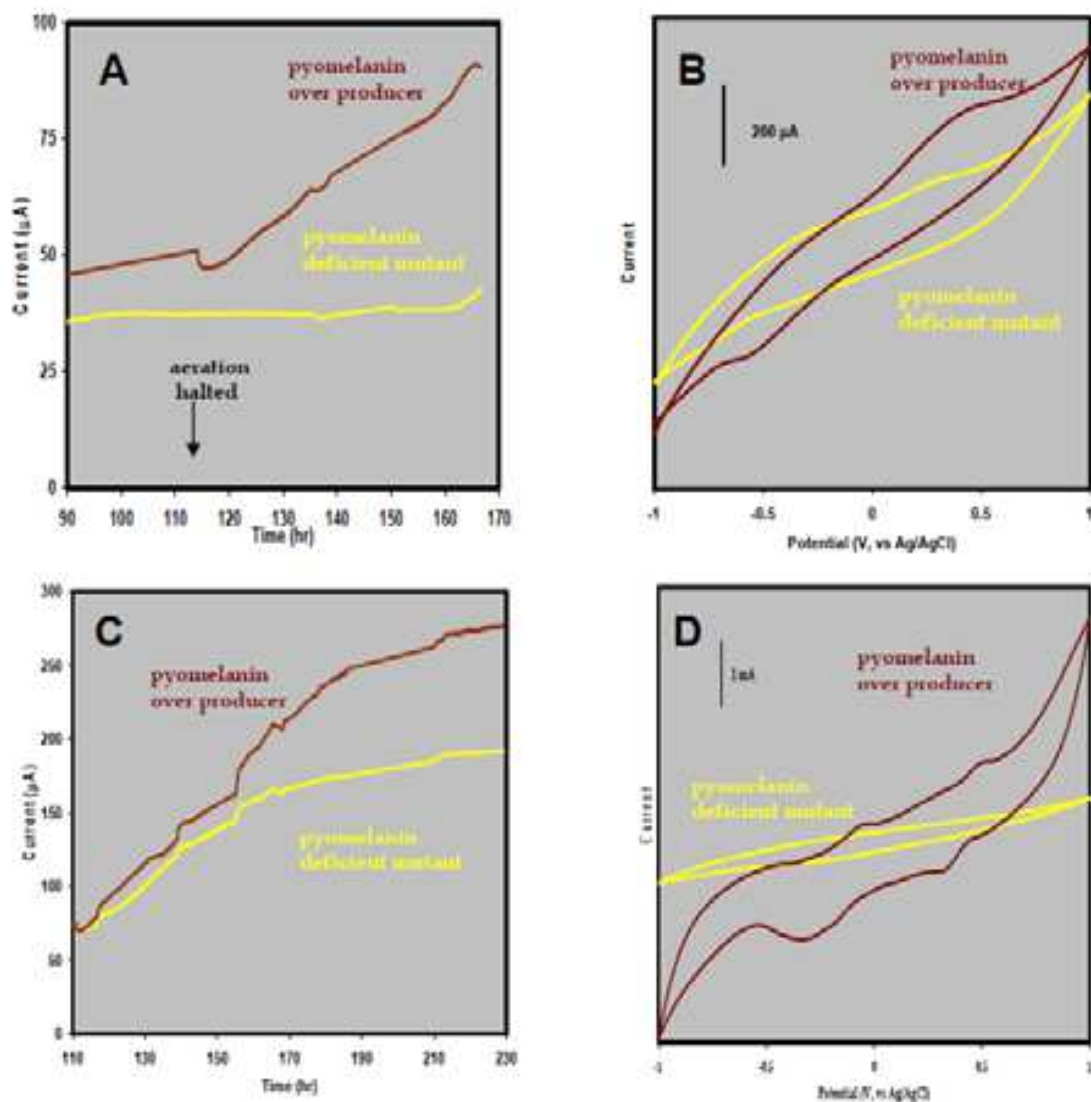


Fig. 16. Affects of pyomelanin production on current generation by bacteria. Current production from initiation of bacterial biofilms on a graphite rod electrode over time (A) increased by the pyomelanin over producer after aeration stopped, likely due to production of pyomelanin under low dissolved oxygen conditions. Cyclic voltammetry (B) demonstrated enhanced current production by the pyomelanin over producer with a current response similar to that of pyomelanin. Current production from established bacterial biofilms on a graphite rod electrode over time (C) increased by the pyomelanin over producer after dissolved oxygen levels dropped. Cyclic voltammetry (D) demonstrated an increase in redox couples and increased current density by the pyomelanin over producer. The increased current density is indicative of higher current production in the biofilm.

## 6. Conclusions and outlook

Biotechnological application of bacterial polymers, including pyomelanin have been discussed (David, et al, 1996; Weiner, 1997). The multifaceted nature of melanin, including pyomelanin offers numerous opportunities for applications, such as reporter genes, cosmetics, dyes, colorings and sunscreens (Weiner, 1997). In this report, we demonstrated

further, the biotechnological utility of pyomelanin. Through the exploitation of its electron transfer properties metal reduction in relation to bioremediation can be enhanced in-situ. Hyper production of pyomelanin may lead to surface sorption by a wide range of microorganisms through interspecies sorption of the soluble polymers, thereby altering redox activity in soil microbial communities. The mineral sorption and metal chelation capacity of pyomelanin has been shown here to enhance contaminant immobilization in soils. As an electron conduit, pyomelanin also has the potential to increase the current response from biofilms for electricity production in microbial fuel cells.

Future applications of pyomelanin could include its use as an extracellular electronic material. A further understanding of the structure of this polymer and its metal chelation behavior will provide valuable insights into how to modify it chemically, potentially for enhanced electrochemical activity. Research into the biochemistry and microbial ecology of pyomelanin production and utilization will allow us to understand its role in the survival of microorganisms of clinical and environmental significance.

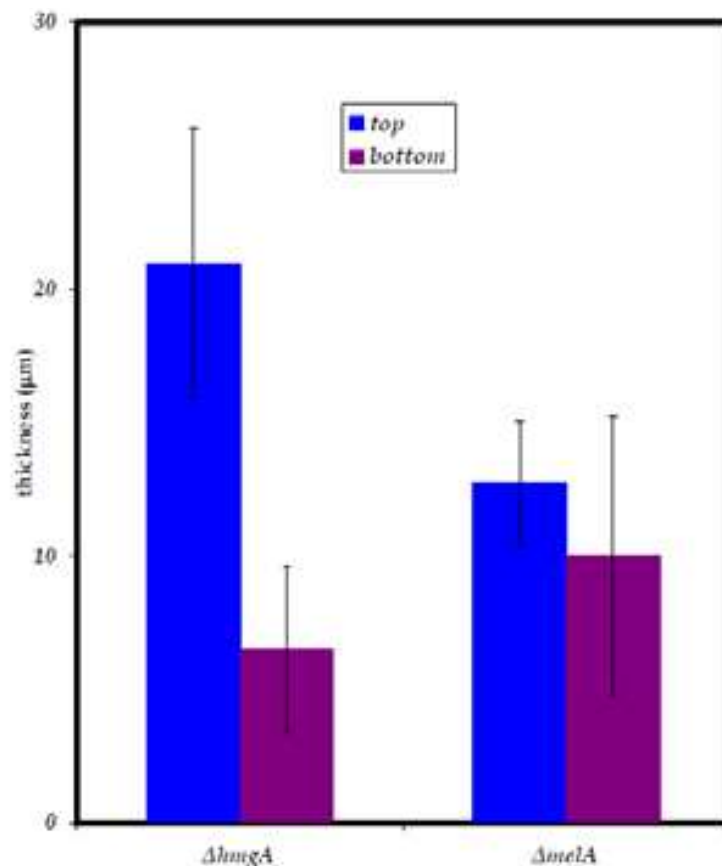


Fig. 17. Biofilm thickness on graphite electrodes. Biofilm thickness on the electrodes (determined with confocal microscopy) was similar for both cultures at the bottom of the 5 cm electrode but thicker at the top (air/medium interface).

## 7. Acknowledgements

This research was supported in part through funding by AES Hatch grant 389: the Department of Energy (DOE) Office of Science NABIR/ERSP and Genomics: GTL programs,

the Savannah River National Laboratory Directed Research and Development Program, and Soil and Groundwater Closure Projects of the Savannah River Site funded through DOE-Environmental Management Program. This document was prepared in conjunction with work accomplished at SRNL under Contract No. DE-AC09-08SR22470 with the US Department of Energy. We would like to thank Dr. M. Duff for XRF analyses and T. Poppy, A. Maloney, W. Jones and Y.G. Kritzas for able technical assistance. We would also like to thank Dr. D.A. Lowy for assistance and valuable discussions in electrochemistry.

## 8. References

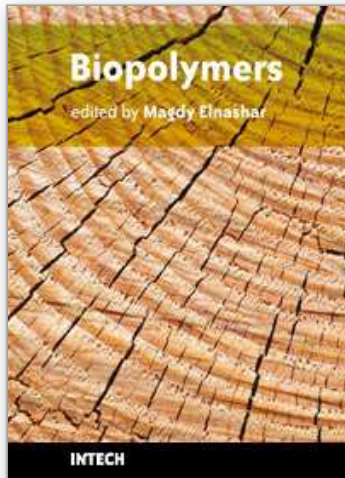
- Beltrán-Valero de Bernabé, D., F.J. Jimenez, R. Aquaron & S. Rodríguez de Córdoba. 1999. Analysis of alkaptonuria (AKU) mutations and polymorphisms reveals that the CCC sequence motif is a mutual hot spot in the homogentisate 1,2 dioxygenase gene (HGO). *Am. J. Hum. Gene.* 64: 1316-1322.
- Boles, B.R., M. Thoendel, & P.K. Singh. 2004. Self-generated diversity produces “insurance effects” in biofilm communities. *Proc. Nat. Acad. Sci.* 101:16630-16635.
- Boles, B.R., & P.K. Singh. 2008. Endogenous oxidative stress produces diversity and adaptability in biofilm communities. *Proc. Nat. Acad. Sci.* 105:12503-12508.
- Chatfield, C.H., & N.P. Cianciotto, 2007. The secreted pyomelanin pigment of *Legionella pneumophila* confers ferric reductase activity. *Infect. Immun.* 75:4062-4070.
- Coon S.L., S. Kotob, B.V. Jarvis, S. Wang, W.C. Fuqua, and R.M. Weiner. 1994. Homogentisic acid is the product of MelA, which mediated melanogenesis in the marine bacterium *Shewanella colwelliana* D. *Appl. Env. Microbiol.* 60:3006-3010.
- Drapcho, C.M, N.M. Nhuan & T.H. Walker. 2008. Microbial Fuel Cells. in *Biofuels Engineering Process Technology*. pp 303-327. (Ed) L.S. Hager. McGraw-Hill Co. New York, NY. USA.
- Ellis, D.H. & D.A. Griffiths. 1974. The location and analysis of melanins in cell walls of some soil fungi. *Can. J. Microbiol.* 20:1379-1386.
- Ehrlich, H.L. 2002. In *Geomicrobiology*. Marcel Decker Inc. N.Y., N.Y., pp 378-380.
- Gadd, G.M., D.J. Gray, & P.J. Newby. 1990. Role of melanin in fungal biosorption of tributyltin chloride. *Applied Microbiology and Biotechnology* 34, 116-121.
- Gadd, G.M. & J.L. Mowll. 1985. Copper uptake by yeast-like cells, hyphae, and chlamydospores of *Aureobasidium pullulans*. *Experimental Mycol.* 9, 230-240.
- Gadd, G.M., C. White, & J.L. Mowll. 1987. Heavy metal uptake by intact cells and protoplasts of *Aureobasidium pullulans*. *FEMS Microbiol. Lett.* 45:261-267.
- Kotob, S.I., S.L. Coon, E.J. Quintero, & R.M. Weiner. 1995. Homogentisic acid is the primary precursor of melanin synthesis in *Vibrio cholera*, a *Hyphomonas* strain, and *Shewanella colwelliana*. *Appl. Environ. Microbiol.* 61:1620-1622.
- Lehman, R.M., F.F. Roberto, D. Earley, D.F. Bruhn, S.E. Brink, S.P. O’Connell, M.E. Delwiche, & F.S. Colwell. 2001. Attached and unattached bacterial communities in a 120-meter corehole in an acidic, crystalline rock aquifer *Appl. Environ. Microbiol.* 67:2095-2106.
- Lehninger AL (1975) Oxidative degradation of amino acids. In: *Biochemistry*. pp.568-570. Worth Publishers. N.Y. NY,
- Lindstedt, S., B. Odelhög, & M. Rundgren. 1977. Purification and some properties of 4-hydroxyphenylpyruvate dioxygenase from *Pseudomonas* sp. P.J. 874. *Biochem.* 16:3369-3377.

- Marsili, E., D.B. Baron, I.D. Shikhare, D. Coursolle, J.A. Gralnick & D.R. Bond. 2008. *Shewanella* secretes flavins that mediate extracellular electron transfer. *Proc. Nat. Acad. Sci.* 105:3968–3973.
- McCuen, P.J. 1988. Culture media components In: *Manual of BBL Products and Laboratory Procedures*. Power, D.A. (ed). Beckton Dickinson Systems, Cockeysville, MD. pp. 293-294.
- McLean, J., O.W. Purvis, B.J. Williamson, & E.H. Bailey. 1998. Role for lichen melanins in uranium remediation. *Nature* 391, 649-650.
- Menter, J.M. & I. Willis. 1997. Electron transfer and photoprotective properties of melanins in solution. *Pigment Cell Res.* 10:214-217.
- Mohan, S.V., G. Mohanakrishna, & P.N. Sarma. 2008. Effect of anodic metabolic function on bioelectricity generation and substrate degradation in single chambered microbial fuel cell. *Environ. Sci. Technol.* 42:8088-8094.
- Nurmi, J.T. & P.G. Tratnyek. 2002. Electrochemical properties of natural organic matter (NOM), fractions of NOM, and model biogeochemical electron shuttles. *Environ. Sci. Technol.* 36:617-624.
- Nyhus, K.J., Wilborn, A.T. & Jacobson E.S. 1997. Ferric iron reduction by *Cryptococcus neoformans*. *Infection and Immunity.* 65:434-438.
- Plonka, P.M. & M. Grabacka. 2006. Melanin synthesis in microorganisms - biotechnical and medical aspects. *ACTA Biochimica Polonica.* 53:429-443.
- Rau, J., H-J. Knackmuss & A. Srolz. 2002. Effects of different quinoide redox mediators on the anaerobic reduction of azo dyes by bacteria *Environ. Sci. Technol.* 36:1497-1504.
- Rodríguez-Rojas, A., A. Mena, S. Martín, N. Borrell, A. Oliver & J. Blázquez. 2009. Inactivation of the *hmgA* gene of *Pseudomonas aeruginosa* leads to pyomelanin hyperproduction, stress resistance and increased persistence in chronic lung infection. *Microbiol.* 155:1050-1057.
- Ruzafa, C., F. Solano, & A. Sanchez-Amat. 1994. The protein encoded by the *Shewanella colwelliana melA* gene is *p*-hydroxyphenylpyruvate dioxygenase. *FEMS Microbiol. Lett.* 124:179-184.
- Schröder, I., E. Johnson & S. deVries. 2003. Microbial ferric iron reductases. *FEMS Microbiol. Rev.* 27:427-447.
- Scott, D.E. & J.P. Martin, in *Humic Substances in Soil and Crop Sciences: Selected Readings*, P. MacCarthy, C.E. Clapp, R.L. Malcolm, and P.R. Bloom, Eds. (Soil Science Society of America, Inc., Madison WI, USA, 1990), chap. 3.
- Steinert, M., M. Flügel, M. Schuppler, J.H. Helgig, A. Supriyono, P. Proksch & P.C. Lück. 2001. The Lyl protein is essential for *p*-hydroxyphenylpyruvate dioxygenase activity in *Legionella pneumophila*. *FEMS Microbiol. Lett.* 203:41-47.
- Steinert, M., H. Engelhard, M. Flügel, E. Wintermeyer & J. Hacker. 1995. The Lyl protein protects *Legionella pneumophila* from light but does not influence its intracellular survival in *Hartmannella vermiformis*. *Appl. Environ. Microbiol.* 61:2428-2430.
- Turick, C.E., L.S. Tisa, & F. Caccavo, Jr. 2002. Melanin production and use as a soluble electron shuttle for Fe(III) oxide reduction and as a terminal electron acceptor by *Shewanella algae* BrY. *Appl. Environ. Microbiol.* 68:2436-2444.
- Turick, C.E., F. Caccavo, Jr., & L.S. Tisa. 2003. Electron transfer to *Shewanella algae* BrY to HFO is mediated by cell-associated melanin. *FEMS Microbiol. Lett.* 220:99-104



- Turick, C.E., A.S. Knox, C. L. Leverette & Y. G. Kritzas. 2008 a. In-situ uranium immobilization by microbial metabolites. Invited paper, J. Environ. Rad. 99:890-899.
- Turick, C.E., F. Caccavo, Jr. & L.S. Tisa. 2008 b. Pyomelanin is Produced by *Shewanella algae* BrY and Affected by Exogenous Iron. Can. J. Microbiol. 54:334-339.
- Turick, C. E. A. Beliaev, A.A. Ekechukwu, T. Poppy, A. Maloney, & D. A. Lowy. 2009. The role of 4-hydroxyphenylpyruvate dioxygenase in enhancement of solid-phase electron transfer by *Shewanella oneidensis* MR-1. FEMS Microbiol. Ecol. 68:223-235.
- White, L.P. 1958. Melanin: A naturally occurring cation exchange material. Nature. 182:1427-1428.
- Yabuuchi, E. & Omyama, A. 1972. Characterization of "pyomelanin"-producing strains of *Pseudomonas aeruginosa*. Internat. J. Syst. Bacteriol. 22:53:64.
- Zatkova, A., D. Beltrán-Valero de Bernabé, H. Polakova, M. Zvarík, E. Feráková, V. Bošák, V. Ferák, L. Kádasi & Rodríguez de Córdoba. 2000. High frequency of alkaptonuria in Slovakia: Evidence for the appearance of multiple mutations in HGO involving different mutational hot spots. Am. J. Hum. Genet. 67:1333-1339.
- Zughaier, S.M., H.C. Ryley, & S.K. Jackson. 1999. A melanin pigment purified from an epidemic strain of *Burkholderia cepacia* attenuates monocyte respiratory burst activity by scavenging superoxide anion. Infect. Immun. 67:908-913.

IntechOpen



## **Biopolymers**

Edited by Magdy Elnashar

ISBN 978-953-307-109-1

Hard cover, 612 pages

**Publisher** Sciyo

**Published online** 28, September, 2010

**Published in print edition** September, 2010

Biopolymers are polymers produced by living organisms. Cellulose, starch, chitin, proteins, peptides, DNA and RNA are all examples of biopolymers. This book comprehensively reviews and compiles information on biopolymers in 30 chapters. The book covers occurrence, synthesis, isolation and production, properties and applications, modification, and the relevant analysis methods to reveal the structures and properties of some biopolymers. This book will hopefully be of help to many scientists, physicians, pharmacists, engineers and other experts in a variety of disciplines, both academic and industrial. It may not only support research and development, but be suitable for teaching as well.

### **How to reference**

In order to correctly reference this scholarly work, feel free to copy and paste the following:

C.E. Turick, A.S. Knox, J.M. Becnel, A.A. Ekechukwu and C.E. Milliken (2010). Properties and Function of Pyomelanin, Biopolymers, Magdy Elnashar (Ed.), ISBN: 978-953-307-109-1, InTech, Available from: <http://www.intechopen.com/books/biopolymers/properties-and-function-of-pyomelanin>

**INTECH**  
open science | open minds

#### **InTech Europe**

University Campus STeP Ri  
Slavka Krautzeka 83/A  
51000 Rijeka, Croatia  
Phone: +385 (51) 770 447  
Fax: +385 (51) 686 166  
[www.intechopen.com](http://www.intechopen.com)

#### **InTech China**

Unit 405, Office Block, Hotel Equatorial Shanghai  
No.65, Yan An Road (West), Shanghai, 200040, China  
中国上海市延安西路65号上海国际贵都大饭店办公楼405单元  
Phone: +86-21-62489820  
Fax: +86-21-62489821

© 2010 The Author(s). Licensee IntechOpen. This chapter is distributed under the terms of the [Creative Commons Attribution-NonCommercial-ShareAlike-3.0 License](https://creativecommons.org/licenses/by-nc-sa/3.0/), which permits use, distribution and reproduction for non-commercial purposes, provided the original is properly cited and derivative works building on this content are distributed under the same license.

IntechOpen

IntechOpen